Rapid Communications

# Constraining the relativistic mean-field model equations of state with gravitational wave observations

Rana Nandi,[1] Prasanta Char,[2] and Subrata Pal[1]

[1]*Department of Nuclear and Atomic Physics, Tata Institute of Fundamental Research, Mumbai 400005, India*

[2]*INFN Sezione di Ferrara, Via Saragat 1, I-44100 Ferrara, Italy*

(Received 19 September 2018; published 22 May 2019)

The first detection of gravitational waves from the binary neutron star merger event GW170817 has started to provide important new constraints on the nuclear equation of state at high density. The tidal deformability bound of GW170817 combined with the observed two solar mass neutron star poses a serious challenge to theoretical formulations of realistic equations of state. We analyze a fully comprehensive set of relativistic nuclear mean-field theories by confronting them with the observational bounds and the measured neutron-skin thickness. We find that only a few models can withstand these bounds which predict a stiff overall equation of state but with a soft neutron-proton symmetry energy. Two possible indications are proposed: Circumstantial evidence of hadron-quark phase transition inside the star and new parametrizations that are consistent with ground-state properties of finite nuclei and observational bounds. Based on extensive analysis of these sets, an upper limit on the radius of a $1.4M_\odot$ neutron star of $R_{1.4} \lesssim 12.9$ km is deduced.

DOI: 10.1103/PhysRevC.99.052802

*Introduction.* The equation of state (EOS) of nuclear matter, characterizing the relation between energy density and pressure of the system, has been the cornerstone in defining the structure of rare isotopes [1], collective properties in nucleus-nucleus collisions [2,3], and structure of a neutron star [4,5]. Yet the predictions of these observables are largely restricted due to incomplete knowledge of the EOS.

While a first-principle calculation of finite density quantum chromodynamics in lattice gauge theory is plagued by the sign problem [6], sophisticated nuclear many-body theories [5,7,8] have served as a promising prospect. These calculations by design reproduce the nuclear matter properties at the saturation density. As a consequence, the lower and higher density predictions of these EOSs are very diverse and remain largely unconstrained. Particularly uncertain is the supranuclear density behavior of nuclear symmetry energy $E_{\rm sym}(\rho)$ and thus the EOS of neutron-rich matter [1,2,4].

The first major observational constraint of the EOS at suprasaturation densities came from the precise measurements of two massive neutron stars (NSs) of masses $(1.928 \pm 0.017)M_\odot$ [9] and $(2.01 \pm 0.04)M_\odot$ [10]. This would effectively exclude unduly soft EOSs where the matter pressure is not sufficient enough to support stars of maximum mass $M_{\rm max} \geqslant 1.97M_\odot$ against gravitational collapse. Conversely, a stiff EOS with large energy density and pressure offers an intriguing possibility to produce exotic phases comprising of hyperons [11,12] and quarks [13].

The historic detection of gravitational waves (GWs) on August 17, 2017, by the LIGO and Virgo collaborations from the binary neutron star (BNS) merger event GW170817 [14] marks the opening of a new possibility to explore the EOS at large densities. The GW signal encodes the information of tidal deformation induced by the strong gravitational field of each star on its companion during the inspiral phase. The tidal deformability, which depends inherently on the properties of the neutron star, can be quantified at the leading order as [15]

$$\Lambda = \frac{2}{3} k_2 \left( \frac{Rc^2}{GM} \right)^5, \tag{1}$$

where $k_2$ is the tidal Love number that depends on the EOS. The large sensitivity of the tidal deformability on the star radius is expected to impose severe constraint on the EOS.

The LIGO and Virgo collaborations inferred a bound on $\Lambda_{1.4} \leqslant 800$ for neutron stars of mass $M = 1.4M_\odot$ from Bayesian analysis of the GW data under the assumption that each star may have a different EOS [14]. Since then, different analysis techniques and model studies were undertaken in an effort to constrain the radii and/or maximum mass of neutron stars and the associated EOSs [16–22] by using the reported $\Lambda_{1.4}$ upper bound. Recently, an improved analysis of these data, using a common EOS for both the stars and with more realistic waveform models, provides $\Lambda_{1.4} = 190^{+390}_{-120}$, which translates into a stringent bound of $\Lambda_{1.4} \leqslant 580$ at the 90% confidence level [23].

Complementary laboratory measurements of skin thickness of neutron-rich heavy nuclei can provide further important checks on the EOS at subsaturation densities [24–26]. Remarkably, the neutron-proton asymmetry pressure that determines the skin in a nucleus of radius $R_{\rm nuc} \approx 10$ fm is essentially the same pressure that dictates the radius $R \approx 10$ km of a neutron star [1]. The Lead Radius Experiment (PREX) measurement at the Jefferson Laboratory [27] for the neutron-skin thickness of $^{208}$Pb, $R^{208}_{\rm skin} = 0.33^{+0.16}_{-0.18}$ fm, may well be employed to impose additional constraints. However, a definitive data-to-theory comparison would require a substantial

 

reduction in the statistical error as planned in the future PREX-II experiment.

The synergy between low- and high-density physics of nuclear matter can be suitably explored using the relativistic mean-field (RMF) theory that provides a natural Lorentz covariant extrapolation from sub- to suprasaturation densities [7,8]. The RMF models offer a comprehensive framework that successfully describes several finite nuclei properties and finds large applications in studies of NS structure.

In this article we have extensively analyzed 269 various EOSs predicted by the RMF models by using the latest observational bounds on neutron stars and measured finite nuclei properties. From the analysis we infer plausible bounds on the radius of neutron stars. We further show that the recent stringent bound on tidal deformability can be reconciled with the appearance of quark phases inside the neutron stars. New relativistic parametric sets are introduced that simultaneously describe the finite nuclei properties and high-density observational constraints.

*Setup.* In the original RMF model [28–30], the interaction between the nucleons is described via the exchange of scalar-isoscalar $\sigma$ mesons and vector-isoscalar $\omega$ mesons. Over the years, the model has been refined by including other mesons (such as vector-isovector $\rho$ mesons and scalar-isovector $\delta$) and introducing nonlinear self-interaction as well as cross-coupling terms for all the mesons [24,31–38].

Based on the form of the interactions in the Lagrangian density, the 269 RMF models [5,7] are broadly recognized as NL-type (with nonlinear $\sigma$ term) [32,34], NL3-type (NL3 and S271 families with additional $\sigma$-$\rho$ and $\omega$-$\rho$ couplings) [31,35], FSU-type (FSU and Z271 families with an additional nonlinear $\omega$ coupling) [36–38], BSR-type (BSR and BSR* families with more nonlinear couplings; BSR does not have nonlinear $\omega$ coupling) [39,40], and DD (with density-dependent couplings) [33]. The associated coupling constants are obtained by sophisticated fitting procedures to the binding energies and charge radii of finite nuclei and/or to the nuclear matter properties at the saturation density $\rho_0$.

The total energy per nucleon, i.e. the EOS, $E(\rho,\delta) = E_0(\rho) + E_{\rm sym}(\rho)\delta^2$, is the sum of the symmetric nuclear matter (SNM) energy per nucleon $E_0(\rho)$ and nuclear symmetry energy $E_{\rm sym}(\rho)$, where $\delta = (\rho_n - \rho_p)/\rho$ is the isospin asymmetry and $\rho_n$, $\rho_p$, and $\rho$ are respectively the neutron, proton and nucleon densities [2,3]. Large-scale comparison [5] of experimental data from finite nuclei and heavy-ion collisions with various model calculations have provided reliable bounds on the incompressibility of SNM, $210 \leqslant K_\infty = 9\rho_0|\partial^2 E/\partial\rho^2|_{\rho_0} \leqslant 280$ MeV, symmetry energy $28 \leqslant E_{\rm sym}(\rho_0) \leqslant 35$ MeV, and its slope parameter $30 \leqslant L = 3\rho_0|\partial E_{\rm sym}(\rho)/\partial\rho|_{\rho_0} \leqslant 87$ MeV at the saturation density $\rho_0$. By imposing these current experimental bounds, 67 RMF models out of 269 sets are found to survive. We will examine the impact of observational bounds and measured neutron-skin thickness on these EOSs without altering the parameters in each model.

*Results.* Figure 1 presents the prediction of tidal deformability $\Lambda_{1.4}$ (for mass $M = 1.4M_\odot$) as a function of maximum mass $M_{\rm max}$ of stars for the 67 RMF EOSs. Models that do not support stars of $M_{\rm max} = 1.97M_\odot$ have essentially a soft

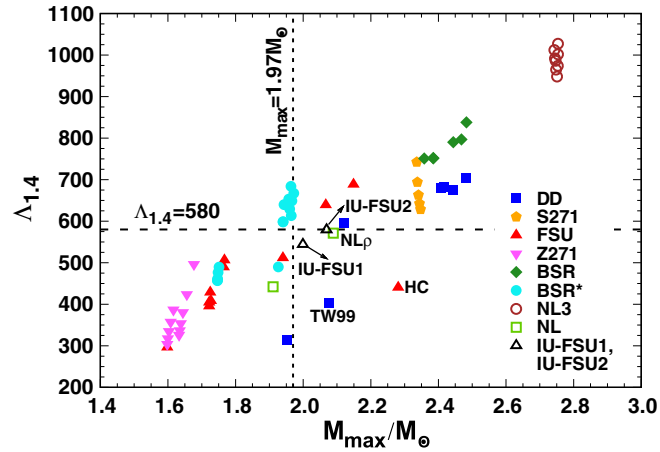


FIG. 1. Tidal deformability $\Lambda_{1.4}$ of neutron star of mass $1.4M_\odot$ vs maximum mass $M_{\rm max}$ for all the RMF EOSs. The horizontal and vertical lines respectively refer to the recent upper bound $\Lambda_{1.4} = 580$ of GW170817 data [23] and lower bound $M_{\rm max} = 1.97M_\odot$ from the observed pulsar PSR J0348+0432 [10].

isospin-symmetric nuclear matter EOS $E_0(\rho)$ which largely dictates NS mass at high density. In contrast, the deformability $\Lambda \approx R^5$ (hence NS radius) is sensitive to the density-dependent symmetry energy $E_{\rm sym}(\rho)$ at $\rho \approx 2\rho_0$. The tidal deformability constraint $\Lambda_{1.4} \leqslant 800$, inferred from the first analysis of the GW170817 event [14], combined with the lower bound on maximum mass, allows a sizable number of RMF EOSs to survive, as can be seen from Fig. 1. The current tight bound on $\Lambda_{1.4} \leqslant 580$ [23] rules out a majority of the EOSs and supports only three existing models with rather soft $E_{\rm sym}(\rho) \approx 46$ MeV at $\rho \approx 2\rho_0$, namely, NL$\rho$ [34] (NL-type EOS with $\sigma$ self-couplings), HC [36] (FSU-type EOS with nonlinear $\omega$, $\rho$), and TW99 [33] (a density-dependent EOS). We also note that the TW99 set provides a tidal deformability of $\Lambda_{1.4} \approx 400$.

To explore the impact of the tidal deformability constraint on the entire structure of a star, we display in Fig. 2 the

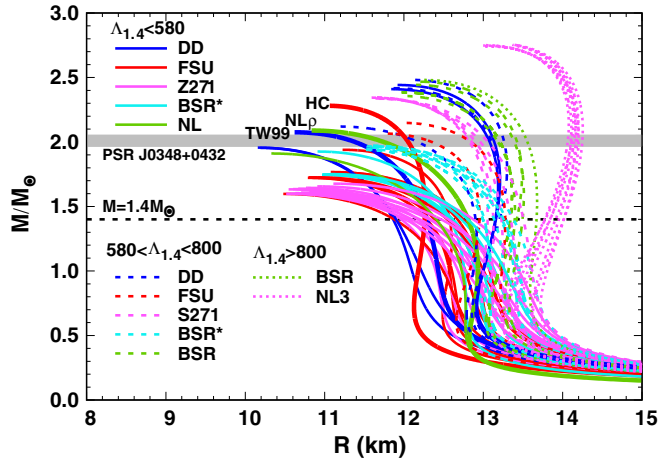


FIG. 2. Mass-radius relation of neutron stars predicted for all the RMF EOSs that fulfill various $\Lambda_{1.4}$ bounds.

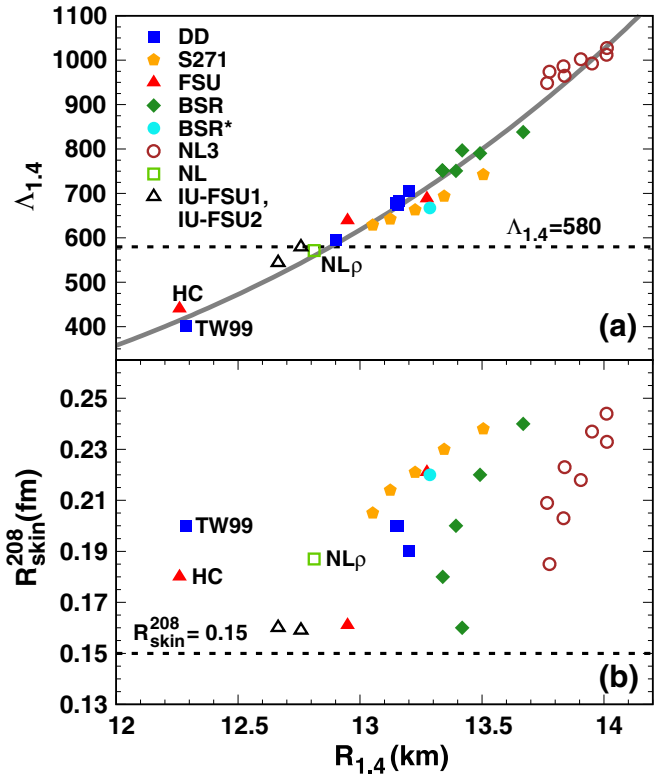


FIG. 3. (a) Correlation between tidal deformability $\Lambda_{1.4}$ and radius $R_{1.4}$ of neutron stars of mass $M = 1.4M_\odot$. The solid line represents the fit $\Lambda_{1.4} = 1.53\times10^{-5}(R_{1.4}/\text{km})^{6.83}$. (b) Correlation between neutron-skin thickness of $^{208}$Pb nuclei $R^{208}_{\text{skin}}$ and $R_{1.4}$. The results are for EOSs that support stars with $M_{\max} \geqslant 1.97M_\odot$.

mass-radius relation of stars for all the EOSs that are subjected to various $\Lambda_{1.4}$ bounds. The resulting correlation between $\Lambda_{1.4}$ and radius $R_{1.4}$ (for a $1.4M_\odot$ star), computed for the EOSs that support maximum mass larger than $1.97M_\odot$, is shown in Fig. 3(a). In general, the increase of $R_{1.4}$ with $\Lambda_{1.4}$ has the natural explanation that $\Lambda$ quantifies the deviation of the gravitational field of a star relative to that of a point-mass object [15]. The exceedingly stiff NL3-type EOSs [31,35] generate stars with large $M_{\max} \approx 2.7M_\odot$ but have fairly large $R_{1.4} \approx 13.7$ km (albeit within a narrow range). Hence, these stars give $\Lambda_{1.4} > 800$ and can be clearly ruled out by the present GW data. Interestingly enough, a bound of $580 < \Lambda_{1.4} < 800$ suggests quite a large variation in the maximum mass $2.0 \lesssim M_{\max}/M_\odot \lesssim 2.5$ but reasonably tight correlation between deformability and radii $12.9 \lesssim R_{1.4}/\text{km} \lesssim 13.50$ for these moderately soft EOSs. A plausible stringent LIGO-Virgo bound $400 \leqslant \Lambda_{1.4} \leqslant 580$ favors EOSs that possess much softer $E_{\text{sym}}(\rho)$ at density $\rho \approx 2\rho_0$. However, due to the super-soft total pressure at high densities, most of these EOSs are excluded by the $M_{\max} \geqslant 1.97M_\odot$ constraint. As also seen in Fig. 1, only three EOSs: NL$\rho$ [34], HC [36], and TW99 [33], are just stiff enough to qualify the combined tidal deformability and maximum mass constraints.

One important upshot of the $M$-$R$ relation of Fig. 2 is the large spread of radius $R_{1.4}$ when all the stars are considered irrespective of their $M_{\max}$. The maximum mass bound [as shown in Fig. 3(a)] enforces a tight correlation of the form $\Lambda_{1.4} = 1.53\times10^{-5}(R_{1.4}/\text{km})^{6.83}$, which suggests the possibility of constraining the radius [18,19] and perhaps the $E_{\text{sym}}(\rho)$. Thus the bound $\Lambda_{1.4} \leqslant 800$, estimated from the first analysis of GW170817 [14], translates to $R_{1.4} \leqslant 13.49$ km, and the recent stringent constraint $\Lambda_{1.4} \leqslant 580$ [23] provides a strict upper limit of $R_{1.4} \leqslant 12.87$ km. Interestingly, the tidal deformability in NL$\rho$ [32] is close to the inferred current upper bound and predicts $R_{1.4} \lesssim 12.81$ km. Albeit, the radius of a NS is known to receive considerable contribution from the low-density crustal equation of state.

It may be mentioned that all 67 RMF EOSs are found to be consistent with the pressure bound at twice the saturation density of $P(2\rho_0) = 3.5^{+2.7}_{-1.7}\times10^{34}$ dyn/cm$^2$ (at the 90% confidence level) as extracted from GW170817 data [23]. Hence, this bound is not very useful to constraining the EOS. In contrast, the bound $P(6\rho_0) = 9.0^{+7.9}_{-2.6}\times10^{35}$ dyn/cm$^2$ at $\rho = 6\rho_0$ rules out overly soft RMF EOSs. However, this estimated bound is more than the central pressures of the binary components of the GW170817 event [23] and therefore should be used with caution.

Complementary and crucial information on $E_{\text{sym}}(\rho)$, i.e., the EOS, at subsaturation densities can be obtained from analysis of skin thickness $R_{\text{skin}} = R_n - R_p$ of nuclei, defined as the difference between the rms radii of neutrons and protons [25,26]. Figure 3(b) shows the correlation between neutron-skin thickness $R^{208}_{\text{skin}}$ of heavy $^{208}$Pb and the stellar radius $R_{1.4}$. A stiff $E_{\text{sym}}(\rho)$ (large slope $L$) induces large values for both the skin and star radius. Although the $R_{\text{skin}}$-$R_{1.4}$ correlation is strong within the same family of EOSs [18], the spread is quite large when all the EOSs from RMF theory are included. This relates to the fact that apart from the slope $L$, the SNM compressibility $K_\infty$ also contributes to the $R_{\text{skin}}$ and NS radius [41]. This also suggests that constraints on symmetry energy and its slope $L$ from measurements of neutron-skin and tidal deformability would be model dependent.

The large statistical uncertainty in the current PREX measurement, $R^{208}_{\text{skin}} = 0.33^{+0.16}_{-0.18}$ fm [27], however, prevents any definite constraint on the EOSs. For reference, we note that while all the parameter sets that predict $R^{208}_{\text{skin}} \approx 0.20$–$0.25$ fm are excluded by the observational $\Lambda_{1.4} < 580$ bound, the three EOSs [33,34,36] allowed by this bound have $R^{208}_{\text{skin}} = 0.18$–$0.20$ fm. Should the future PREX-II experiment confirm the central value of skin thickness $R^{208}_{\text{skin}} > 0.20$ fm with a significantly small statistical error as envisioned, then the observationally constrained EOSs NL$\rho$, TW99, and HC would be excluded.

Any parametric EOS, designed to reproduce nuclear matter properties, should also give a good description of finite nuclei properties. To ascertain this, we have calculated the binding energies and charge radii of some light and heavy nuclei for the three parameter sets that satisfy both the observational bounds. The TW99 set which was obtained by including the saturation properties of nuclear matter as well as binding energies of some finite nuclei in the fitting protocol obviously has the best agreement as seen in Fig. 4. In contrast, the other two sets (HC and NL$\rho$) which have been fitted to only the nuclear matter saturation properties, fail to provide reasonable description of finite nuclei properties.

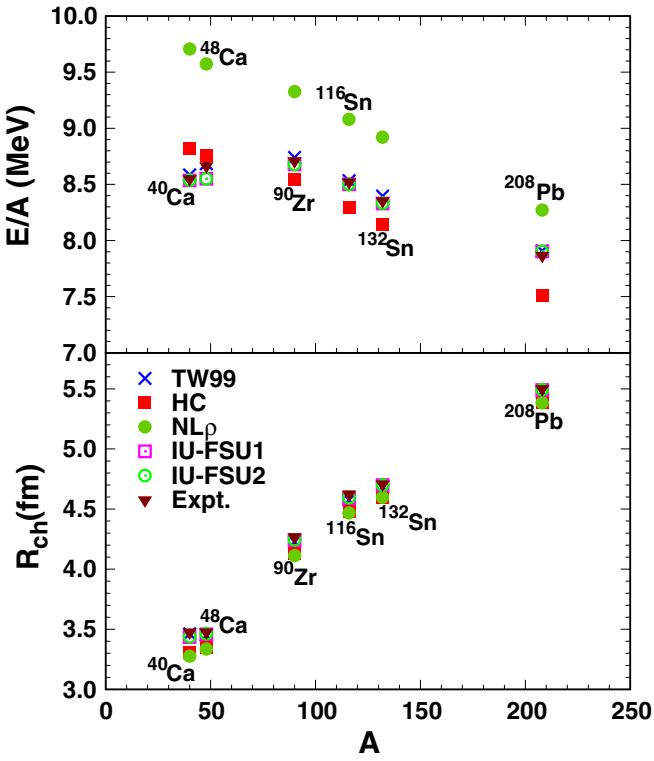


FIG. 4. Binding energy and charge radius of nuclei calculated for viable RMF sets and compared with data; see text for details.

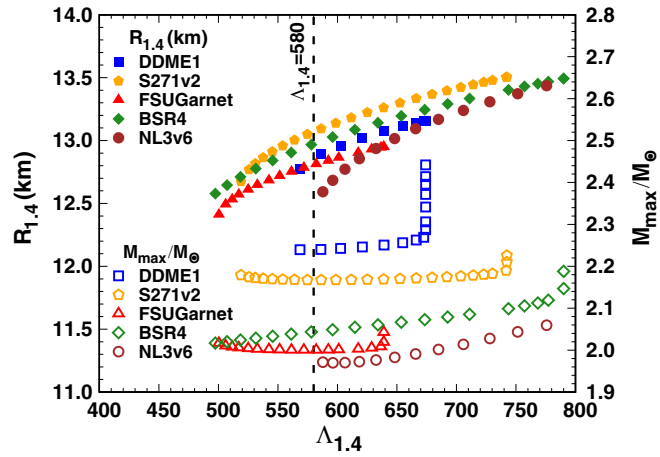


FIG. 5. Correlations between $R_{1.4}$ and $\Lambda_{1.4}$ (left scale) and $M_{\max}$ and $\Lambda_{1.4}$ (right scale) for EOSs with hadron-quark phase transition constructed from the RMF model for the hadronic phase and bag model for the quark phase. In each individual RMF set shown, the bag parameter is varied [21] to generate different EOSs with first-order phase transition using Gibbs conditions.

*Implications.* Various parametrizations of the RMF model have been generated in the last five decades that are consistent with nuclear and neutron star properties. The tension of RMF models with the current observational data poses intriguing questions: Are the GW data an evidence of exotic phases such as quarks inside the NS? Is there still scope to devise new parameter sets by accommodating all the constraints? We will next explore these interesting possibilities.

The gravitational waves from the merger of binary neutron stars have the potential to investigate the possible existence of a deconfined quark phase at high densities [20,42–44]. The appearance of quarks (or any new degrees of freedom) inside the star at $\rho > \rho_0$ softens the EOS, resulting in a decrease of $M_{\max}$ and radius. Thus a hadronic EOS which produces $M_{\max} \gtrsim 2M_\odot$ for a neutron star could be a possible candidate for the inclusion of exotic phases. Such hadronic EOSs can be identified by inspection of Fig. 2.

A phase transition from hadron to quark matter in the NS interior, consistent with the earlier $\Lambda_{1.4} \leqslant 800$ constraint, was recently shown to prevail [21] for realistic parameters in the bag model that provides a phenomenological description of the quark phase [45]. Following the methodology described in Ref. [21], we generated EOSs with phase transition by considering one representative hadronic EOS from each family of RMF models that gives $M_{\max} \geqslant 1.97M_\odot$ and by continuously varying the bag pressure in the range $B_{\rm eff}^{1/4} \simeq 145$–$200$ MeV. A small value of $B_{\rm eff}^{1/4}$ causes early appearance of the quark phase resulting in small $M_{\max}$ and $R_{1.4}$. Figure 5 illustrates the $\Lambda_{1.4}$-$R_{1.4}$ and $\Lambda_{1.4}$-$M_{\max}$ correlations obtained from these EOSs with hadron-quark phase transition. Remarkably, for all these hadronic EOSs (except for NL3v6) we find a range of bag pressures which are consistent with the stringent bound of $\Lambda_{1.4} \leqslant 580$ and maximum mass constraint—a possible indication of quark-hadron phase transition in the neutron star core. Moreover, these EOSs predict a radius of $R_{1.4} \lesssim 12.94$ km close to that found from pure hadronic EOSs.

Finally, we demonstrate how one can generate new EOSs consistent with both the observational and experimental data. Let us consider the original IU-FSU parameter set [46] which provides a good description of finite nuclei and nuclear saturation properties. We recall that the model predicts $\Lambda_{1.4} \simeq 512$, well within the GW170817 bound, and $M_{\max} = 1.94M_\odot$ slightly below the $M_{\max}$ constraint. The nonlinear self-coupling term for the $\omega$ meson, with coupling constant $\zeta = 0.03$, mainly determines the stiffness of EOS at high densities [46]. By fine tuning $\zeta$ to 0.025 and 0.020, for example, and refitting other parameters to reproduce the nuclear properties at $\rho_0$, we construct two new parameter sets: IU-FSU1 and IU-FSU2. Both these sets now generate $M_{\max} > 1.97M_\odot$ and $\Lambda_{1.4} < 580$. The resulting correlations involving $\Lambda_{1.4}$ with $M_{\max}$ and $R_{1.4}$ are displayed in Figs. 1 and 3. As expected, these new sets provide reasonable description of finite nuclear properties as shown in Fig. 4. Interestingly, the NS radii for IU-FSU1 and NL$\rho$ nearly match, which may suggest that the $\Lambda_{1.4} \leqslant 580$ bound translates into $R_{1.4} \lesssim 12.81$ km.

*Conclusions.* We have employed observational data from the gravitational-wave event GW170817 and neutron star mass $M_{\max} \geqslant 1.97M_\odot$ in conjunction with laboratory measurements of neutron skin thickness to constrain the EOSs within RMF theory. The maximum mass bound excludes several EOSs that predict diverse values of NS radius and provides a tight correlation between $R_{1.4}$ and $\Lambda_{1.4}$. Whereas, the

first inferred bound $\Lambda_{1.4} \leqslant 800$ translates to a NS radius with an upper limit $R_{1.4} < 13.50$ km, the recent improved bound $\Lambda_{1.4} \leqslant 580$ provides $R_{1.4} < 12.88$ km. The strict bound on $\Lambda_{1.4}$ rules out all EOSs, but a few with soft $E_{\rm sym}$ at density $\rho \approx 2\rho_0$. If stars have hadron to quark phase transitions, several EOSs are shown to be consistent with all the measured bounds. Complementary precise estimate of skin thickness of nuclei that is sensitive to the slope of $E_{\rm sym}$ should provide further important checks.

It may be noted that though the phenomenological RMF approach provides a reasonable description of the EOS over a wide density range, it does not incorporate the realistic microscopic many-body nuclear interactions [47,48]. Moreover, the RMF models do not contain the essential features of a strong interaction described by QCD such as chiral symmetry and broken scale invariance [49] at finite nuclear matter densities. It will be interesting to compare our predictions obtained within the RMF models with those in the microscopic models.


[1] B. A. Brown, Phys. Rev. Lett. **85**, 5296 (2000).
[2] B. A. Li, L. W. Chen, and C. M. Ko, Phys. Rep. **464**, 113 (2008).
[3] M. B. Tsang, Y. Zhang, P. Danielewicz, M. Famiano, Z. Li, W. G. Lynch, and A. W. Steiner, Phys. Rev. Lett. **102**, 122701 (2009).
[4] J. M. Lattimer and M. Prakash, Science **304**, 536 (2004).
[5] M. Oertel, M. Hempel, T. Klähn, and S. Typel, Rev. Mod. Phys. **89**, 015007 (2017).
[6] P. de Forcrand, PoS LAT **2009**, 010 (2009).
[7] M. Dutra, O. Lourenço, S. S. Avancini, B. V. Carlson, A. Delfino, D. P. Menezes, C. Providência, S. Typel, and J. R. Stone, Phys. Rev. C **90**, 055203 (2014).
[8] J. M. Lattimer and M. Prakash, Phys. Rep. **621**, 127 (2016).
[9] E. Fonseca *et al.*, Astrophys. J. **832**, 167 (2016).
[10] J. Antoniadis *et al.*, Science **340**, 1233232 (2013).
[11] K. A. Maslov, E. E. Kolomeitsev, and D. N. Voskresensky, Phys. Lett. B **748**, 369 (2015).
[12] P. Char, S. Banik, and D. Bandyopadhyay, Astrophys. J. **809**, 116 (2015).
[13] M. Alford, M. Braby, M. W. Paris, and S. Reddy, Astrophys. J. **629**, 969 (2005).
[14] B. P. Abbott *et al.* (LIGO Scientific and Virgo Collaborations), Phys. Rev. Lett. **119**, 161101 (2017).
[15] T. Hinderer, B. D. Lackey, R. N. Lang, and J. S. Read, Phys. Rev. D **81**, 123016 (2010).
[16] B. Margalit and B. D. Metzger, Astrophys. J. **850**, L19 (2017).
[17] D. Radice, A. Perego, F. Zappa, and S. Bernuzzi, Astrophys. J. **852**, L29 (2018).
[18] F. J. Fattoyev, J. Piekarewicz, and C. J. Horowitz, Phys. Rev. Lett. **120**, 172702 (2018).
[19] E. Annala, T. Gorda, A. Kurkela, and A. Vuorinen, Phys. Rev. Lett. **120**, 172703 (2018).
[20] E. R. Most, L. R. Weih, L. Rezzolla, and J. Schaffner-Bielich, Phys. Rev. Lett. **120**, 261103 (2018).
[21] R. Nandi and P. Char, Astrophys. J. **857**, 12 (2018).
[22] N. B. Zhang, B. A. Li, and J. Xu, Astrophys. J. **859**, 90 (2018).
[23] B. P. Abbott *et al.* (LIGO Scientific and Virgo Collaborations), Phys. Rev. Lett. **121**, 161101 (2018).
[24] C. J. Horowitz and J. Piekarewicz, Phys. Rev. Lett. **86**, 5647 (2001).
[25] X. Roca-Maza, M. Centelles, X. Vinas, and M. Warda, Phys. Rev. Lett. **106**, 252501 (2011).
[26] B. K. Sharma and S. Pal, Phys. Lett. B **682**, 23 (2009).
[27] S. Abrahamyan *et al.* (PREX Collaboration), Phys. Rev. Lett. **108**, 112502 (2012).
[28] J. D. Walecka, Ann. Phys. (NY) **83**, 491 (1974).
[29] J. Boguta and A. R. Bodmer, Nucl. Phys. A **292**, 413 (1977).
[30] B. D. Serot and J. D. Walecka, Int. J. Mod. Phys. E **06**, 515 (1997).
[31] G. A. Lalazissis, J. Konig, and P. Ring, Phys. Rev. C **55**, 540 (1997).
[32] M. Centelles, M. Del Estal, and X. Vinas, Nucl. Phys. A **635**, 193 (1998).
[33] S. Typel and H. H. Wolter, Nucl. Phys. A **656**, 331 (1999).
[34] B. Liu, V. Greco, V. Baran, M. Colonna, and M. Di Toro, Phys. Rev. C **65**, 045201 (2002).
[35] C. J. Horowitz and J. Piekarewicz, Phys. Rev. C **66**, 055803 (2002).
[36] J. K. Bunta and S. Gmuca, Phys. Rev. C **68**, 054318 (2003).
[37] B. G. Todd-Rutel and J. Piekarewicz, Phys. Rev. Lett. **95**, 122501 (2005).
[38] W. C. Chen and J. Piekarewicz, Phys. Lett. B **748**, 284 (2015).
[39] S. K. Dhiman, R. Kumar, and B. K. Agrawal, Phys. Rev. C **76**, 045801 (2007).
[40] B. K. Agrawal, Phys. Rev. C **81**, 034323 (2010).
[41] M. Fortin, C. Providencia, A. R. Raduta, F. Gulminelli, J. L. Zdunik, P. Haensel, and M. Bejger, Phys. Rev. C **94**, 035804 (2016).
[42] D. Radice, S. Bernuzzi, W. Del Pozzo, L. F. Roberts, and C. D. Ott, Astrophys. J. **842**, L10 (2017).
[43] E. R. Most, L. J. Papenfort, V. Dexheimer, M. Hanauske, S. Schramm, H. Stocker, and L. Rezzolla, Phys. Rev. Lett. **122**, 061101 (2019).
[44] A. Bauswein, N. U. F. Bastian, D. B. Blaschke, K. Chatziioannou, J. A. Clark, T. Fischer, and M. Oertel, Phys. Rev. Lett. **122**, 061102 (2019).
[45] D. Bandyopadhyay, S. Chakrabarty, and S. Pal, Phys. Rev. Lett. **79**, 2176 (1997).
[46] F. J. Fattoyev, C. J. Horowitz, J. Piekarewicz, and G. Shen, Phys. Rev. C **82**, 055803 (2010).
[47] K. Hebeler, J. M. Lattimer, C. J. Pethick, and A. Schwenk, Phys. Rev. Lett. **105**, 161102 (2010).
[48] E. Rrapaj, A. Roggero, and J. W. Holt, Phys. Rev. C **93**, 065801 (2016).
[49] M. Hanauske, D. Zschiesche, S. Pal, S. Schramm, H. Stoecker, and W. Greiner, Astrophys. J. **537**, 958 (2000).